HILDEBRANDT, G., STEPHENSON, J. D. & WAGENFELD, H. (1975). *Z. Naturforsch. Teil A*, **30**, 697-707.
HUBBELL, J. H. (1969). *Photon Cross Sections, Attenuation Coefficients, and Energy Absorption Coefficients from* 10 keV *to* 100 GeV. Report NSRDS-NBS 29. Gaithersburg: National Bureau of Standards.
HUBBELL, J. H. (1971). *At. Data*, **3**, 241-297.
HUBBELL, J. H. (1982). *Int. J. Appl. Radiat. Isot.* **33**, 1269-1290.
HUBBELL, J. H., MCMASTER, W. H., DEL GRANDE, N. K. & MALLETT, J. H. (1974). *International Tables for X-ray Crystallography*, Vol. IV, pp. 47-70. Birmingham: Kynoch Press. (Present distributor D. Reidel, Dordrecht.)
HUBBELL, J. H. & ØVERBØ, I. (1979). *J. Phys. Chem. Ref. Data*, **8**, 69-105.
HUBBELL, J. H., VEIGELE, W. J., BRIGGS, E. A., BROWN, R. T., CROMER, D. T. & HOWERTON, R. J. (1975). *J. Phys. Chem. Ref. Data*, **4**, 471-538; erratum: *J. Phys. Chem. Ref. Data* (1977). **6**, 615-616.
International Tables for X-ray Crystallography (1974). Vol. IV. Birmingham: Kynoch Press. (Present distributor D. Reidel, Dordrecht.)
JACKSON, D. F. & HAWKES, D. J. (1981). *Phys. Rep.* **70**, 169-233.
KIRBY, R. K., HAHN, T. A. & ROTHROCK, B. D. (1972). *American Institute of Physics Handbook*, 3rd ed., p. 4-129. New York: McGraw-Hill.
KLUG, H. P. & ALEXANDER, L. E. (1973). *X-ray Diffraction Procedures*, 2nd ed., pp. 271-417. New York: John Wiley & Sons.
KOCH, B., MACGILLAVRY, C. H. & MILLEDGE, H. J. (1962). *International Tables for X-ray Crystallography*, Vol. III, pp. 157-192. Birmingham: Kynoch Press. (Present distributor D. Reidel, Dordrecht.)
LANG, A. R. (1958). *J. Appl. Phys.* **29**, 597-598.
LAWRENCE, J. L. (1977). *Acta Cryst.* A**33**, 343.
LEROUX, J. & THINH, T. P. (1977). *Revised Tables of X-ray Mass Attenuation Coefficients*. Quebec: Corporation Scientifique Claisse, Inc.
LIEBHAFSKY, H. A., PFEIFFER, H. G., WINSLOW, E. H. & ZEMANY, P. D. (1960). *X-ray Absorption and Emission in Analytical Chemistry*, pp. 313-317. New York: John Wiley & Sons.
MCMASTER, W. H., DEL GRANDE, N. K., MALLETT, J. H. & HUBBELL, J. H. (1969, 1970). *Compilation of X-ray Cross Sections*. Report UCRL-50174. (Section I, 1970; Section II, 1969; Section III, 1969; Section IV, 1969). Lawrence Livermore National Laboratory, Livermore, California.
MARCO, J. J. DE & SUORTTI, P. (1971). *Phys. Rev. B*, **4**, 1028-1033.
MIKA, J. F., MARTIN, L. J. & BARNEA, Z. (1985). *J. Phys. C*, **18**, 5215-5223.
MONTENEGRO, E. C., BAPTISTA, G. B. & DUARTE, P. W. E. P. (1978). *At. Data Nucl. Data Tables*, **22**, 131-177.
NORDFORS, B. (1960). *Ark. Fys.* **18**, 37-47.
PLECHATY, E. F., CULLEN, E. E. & HOWERTON, R. J. (1981). *Tables and Graphs of Photon-Interaction Cross-Sections from* 0·1 keV *to* 100 MeV *Derived from the LLL Evaluated-Nuclear-Data Library*. Report UCRL-50400, Vol. 6, Rev. 3. Lawrence Livermore National Laboratory, Livermore, California.
RÖNTGEN, W. C. (1895). *Sitzungsber. Würzburger Physik.-Medic. Gesellschaft.*
SANO, H., OHTAKA, K. & OHTSUKI, Y. H. (1969). *J. Phys. Soc. Jpn*, **27**, 1254-1261.
SCHAUPP, D., SCHUMACHER, M., SMEND, F., RULLHUSEN, P. & HUBBELL, J. H. (1983). *J. Phys. Chem. Ref. Data*, **12**, 467-512.
SCOFIELD, J. H. (1973). *Theoretical Photoionization Cross Sections from* 1 *to* 1500 keV. Report UCRL-51326. Lawrence Livermore National Laboratory, Livermore, California.
STORM, E. & ISRAEL, H. I. (1970). *Nucl. Data Tables*, A**7**, 565-681.
THEISEN, R. & VOLLATH, D. (1967). *Tables of X-ray Mass Attenuation Coefficients*. Düsseldorf: Verlag Stahleisen.
VEIGELE, W. J. (1973). *At. Data*, **5**, 51-111.
VICTOREEN, J. A. (1949). *J. Appl. Phys.* **20**, 1141-1147.

Acta Cryst. (1987). A**43**, 112-117

Maximum Entropy Solution of a Small Centrosymmetric Crystal Structure

BY S. F. GULL, A. K. LIVESEY* AND D. S. SIVIA

Cavendish Laboratory, University of Cambridge, Madingley Road, Cambridge CB3 0HE, England

(*Received* 27 *February* 1986; *accepted* 22 *July* 1986)

Abstract

The maximum entropy (MAXENT) method has been used *ab initio* to solve a previously determined small centrosymmetric crystal structure, bis(acetylacetonato)dichlorotin, $C_{10}H_{14}Cl_7O_4Sn$ [Miller & Schlemper (1978). *Inorg. Chim. Acta*, **30**, 131-134; Webster & Wood (1981). *J. Chem. Res.* (*M*), pp. 0450-0456]. The resulting electron density maps are of a very high quality, comparable or even superior to the conventional maps calculated from the refined phases. The method, therefore, holds good promise for the solution of larger and more difficult structures. The addition of simple chemical and symmetry information about the heavy atoms in the structure greatly improves the reconstruction and shows the capability of MAXENT to solve structures from partial fragments.

1. Introduction

Although the theory of solving the phaseless Fourier transform problem by means of the maximum entropy (MAXENT) method has been extensively discussed (Collins, 1982; Steenstrup & Wilkins, 1984; Bricogne, 1984; Livesey & Skilling, 1985; Navassa, 1985; and

* Present address: Department of Applied Mathematics and Theoretical Physics, Silver Street, Cambridge, and Medical Research Council, Hills Road, Cambridge.

0108-7673/87/010112-06$01.50

references therein), there have been few practical demonstrations of its use in crystallography. The difficulty is due partly to the non-quadratic behaviour of the Shannon-Jaynes entropy, but mainly to the multiple local maxima in this function when only intensity data are available. The Shannon-Jaynes entropy (Jaynes, 1983) is given by

$$S = -\sum p_i \log (p_i/m_i)$$

where $p_i = \rho_i/\sum \rho_i$ is the proportion of the electron density ρ in pixel i, and m_i is a 'measure', or default model, which encodes any prior knowledge about the position of the atoms. In the absence of such knowledge the $\{m_i\}$ are all set equal.

Given information about the amplitudes of the structure factor we can set up a constraint function (Gull & Daniell, 1978; Livesey & Skilling, 1985):

$$C = \sum_{k=1}^{M} \frac{(|F_k| - |D_k|)^2}{\sigma_k^2}$$

where D_k is the observed magnitude of the kth structure factor, F_k is the calculated magnitude of the kth structure factor for a trial map $\{\rho_i\}$, σ_k^2 is the variance of the kth observed structure factor, and M is the number of observed structure factors.

If the value of this constraint function is low enough ($\leq M$), then our trial electron density map yield structure factors in statistical agreement with the data. Our final MAXENT solution is that map which maximizes S under the constraint $C \leq M$. In this formulation, centrosymmetric reflections are particularly difficult to handle because for a reflection to change sign during refinement its amplitude must pass through zero and thereby invokes a high penalty in the constraint function. In contrast, complex structure factors are able to rotate their phases at constant amplitude and hence constant C.

In this paper, we report the *ab initio* solution of a small heavy-atom centrosymmetric structure $C_{10}H_{14}Cl_2O_4Sn$ (TICLAC). Similar structures can, of course, be routinely solved by Patterson or direct methods, but our aims were: (1) To show clearly the close correspondence between direct methods and MAXENT, formally proved by Bricogne (1984). (2) To gain some understanding of the complexity of the phase-branching structure. (3) To test the ability of MAXENT to extend phases about heavy atoms.

The second part of the investigation tested the ability of MAXENT to incorporate recognized fragments of the structure into the phase-determining procedure and thereby improve the images of the electron density in the crystal.

Finally, we hoped to find MAXENT images of the high quality that we have come to expect in other fields of science (for a review see Gull & Skilling, 1984).

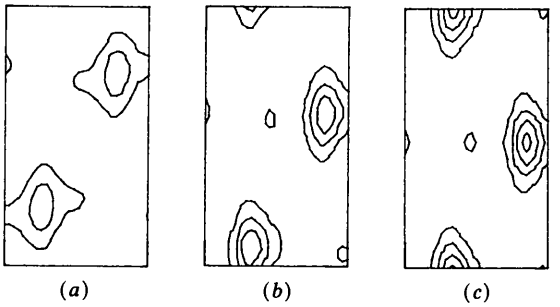

Fig. 1. Figs. 1-6 show sections through the unit cell at various stages of the MAXENT *ab initio* reconstruction calculated on a $32\times32\times32$ pixel grid. In all cases, (*a*) section 1, (*b*) section 6, (*c*) section 9. The reconstruction from the starting set: F_{000}, $F_{11\bar{1}}$, F_{021}. [Contour levels (e Å^{-3}): Figs. 1 to 5: 0·75, 1·5, 2·25, 3·00; 6, 32, 58, 84, 110. Fig. 6: −0·70, −0·35, 0, 0·35, 0·75, 1·05, 1·40; 1·7, 3·4, 5·1, 6·8.]

2. The *ab initio* solution

TICLAC crystallizes in space group $C2/c$ with $a = 13{\cdot}965$, $b = 7{\cdot}889$, $c = 13{\cdot}805$ Å, $\beta = 107{\cdot}55°$ and $Z = 4$. Webster & Wood (1981) report the structure, which was initially solved by Miller & Schlemper (1978), and give an amusing explanation for its perverse name (suggestive of a titanium compound!). Our calculations used a $32\times32\times32$ pixel grid (for the whole unit cell), but only a subset of structure factors ($|h|, |k|, |l| \leq 5$) so as to reduce the size of the computation.

In order to define the origin, two strong low-angle reflections ($11\bar{1}$, $U = 0{\cdot}31$ and 021, $U = 0{\cdot}16$), had arbitrary phases assigned (0 and π, respectively). The data are then linear functions of the electron density and the Cambridge MAXENT algorithm (Skilling & Bryan, 1984) was used to form the MAXENT map from these (unique) reflections alone. This is displayed in Fig. 1.

The MAXENT map predicts the amplitudes and phases of Fourier components not yet included, and the strongest of these are listed in Table 1. The largest amplitudes (and hence the strongest phase indications) occur for those reflections forming triplets with the origin-defining set. The next strongest group of phase indications arise from quartet relationships, and so on. There is, however, one exception in that the reflection 040 can be formed as a triplet relation both from the 021 and $02\bar{1}$ reflections and from 020, which was already present as a strong Fourier component in the map. These predict opposite signs for the phase of 040 which is therefore expected to be a weak prediction. So far, this is in complete agreement with the theory of direct methods, which uses the triplet and quartets explicitly. *MAXENT*, however, naturally takes into account the effect of quintets, sextets and all higher-order relationships. Although these relationships are weak at this stage of the analysis, far more high-order relationships can be formed than low-order ones, so their cumulative effect

Table 1. *Amplitude and phase predictions of the MAXENT solution using only the origin-defining set of reflections*

			$U(hkl)$	
	Starting set (Origin fixing)	000	1·00	
		11$\bar{1}$	0·31	
		021	0·16	
HKL	MAXENT predictions (U's)	True value (U's)	Relation	True phase?
20$\bar{2}$	−0·15	−0·37	Triplet	Yes
020†	−0·14	−0·17	Triplet	Yes
22$\bar{2}$†	0·07	0·01	Triplet	Yes
13$\bar{2}$†	0·06	−0·06	Triplet	No
130†	0·06	0·07	Triplet	Yes
11$\bar{2}$†	0·06	0·12	Triplet	Yes
110†	−0·06	−0·03	Triplet	Yes
31$\bar{3}$	−0·03	−0·19	Quartet	Yes
041	−0·02	−0·19	Quartet	Yes
22$\bar{3}$	0·02	0·16	Quartet	Yes
22$\bar{1}$	−0·02	0·20	Quartet	No
040	−0·02	0·27	Tri+Quin*	No
13$\bar{1}$	−0·02	−0·08	Quartet	Yes
24$\bar{1}$	0·01	0·10	Quartet	Yes
24$\bar{3}$	−0·01	0·03	Quartet	No
33$\bar{2}$†	−0·005	0·002	Quartet	?
31$\bar{2}$	0·003	0·02	Quartet	Yes

U_{hkl} here are defined as $|F_{hkl}|/F_{000}$. No attempt is made to correct for the atomic form factor, nor for the thermal Debye-Waller factors.

* The 040 reflection forms triplets with both 021 (which is in the starting set) and 020 (which is already a strong component of the MAXENT map). These phase indications are contradictory, so the MAXENT prediction is weak.

† New structure factors included in the second cycle.

becomes important when many reflections are considered.

Structure factors with predicted amplitudes that were greater than half of their measured values were then used together with the origin-defininig set to form a new map. The phases were set to the values predicted by the previous map. Of the seven amplitudes included at this stage only one, 13$\bar{2}$, was seriously in error (the measured amplitude of another reflection 33$\bar{2}$ is so small that it can readily change sign). The new map predicted further strong phase indications: these new reflections were then included to form a new map, and so on.

Fig. 2 shows the map after four cycles of this phase-determination procedure when 27 unique structure factors had been included. The Sn atoms have been unambiguously located and there is some indication of the octahedral coordination of the Cl and O atoms around Sn. Fig. 3 shows the map made from 72 unique reflections. The Cl and O atoms are now clearly visible and there is some weak structure at the position of the carbon chain. The map reconstructed from 159 unique reflections with $|h|, |k|, |l| \leq 5$ is displayed in Fig. 4. We refer to these maps as 'phaseless' since they were calculated without any knowledge of the refined phases. For comparison, the MAXENT reconstruction from these reflections using calculated ('true') phases is shown as Fig. 5, and Fig. 6 is the 'conventional' electron density map derived from the same amplitude and phases.

The 'phaseless' and phased reconstructions are very similar. All the atoms are correctly located, with the following exceptions: In the first section of the phaseless map (see Fig. 4) there are two extra maxima, although these would be rejected as chemically meaningless when interpreting the structure in terms of atoms. The extra maxima occurring in section 6, however, appear at first sight to be chemically feasible if they represent C atoms which are hydrogen bonded to the negatively charged Cl atom. The conventional map shows how these features arose. The first section of the conventional map contains stronger truncation ripples than true peaks and so this subset of the structure factors is not sufficient to determine the structure in this plane. At the position of the 'extra atom' found in section 6 there is a severe positive truncation ripple. Although the maximum-entropy

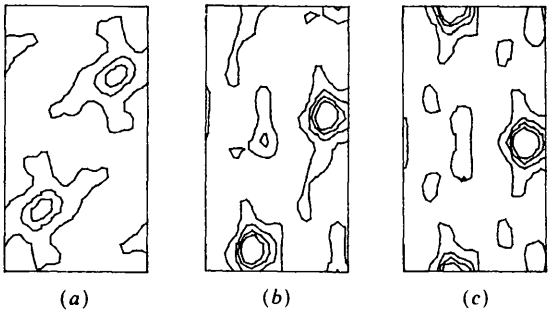

Fig. 2. The reconstruction after four cycles when 27 unique amplitudes had been included.

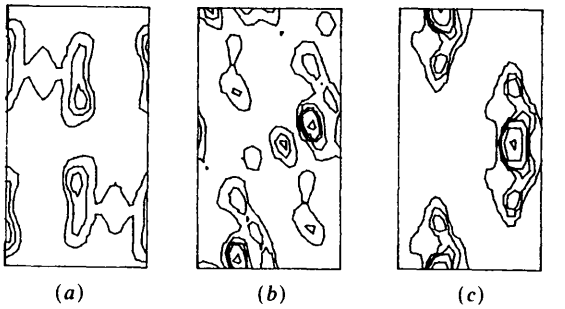

Fig. 3. The reconstruction when 72 amplitudes had been included.

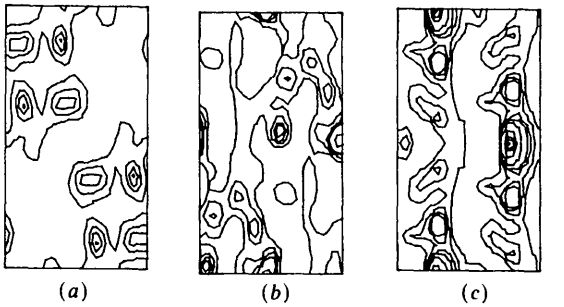

Fig. 4. The final *ab initio* reconstruction from 159 amplitudes.

algorithm strongly attenuates truncation ripples (Gull & Daniell, 1978), it does not remove them entirely. Presumably, the program latched onto this spurious feature, creating a false phase-extension path. Subsequent investigation has suggested that the artefact was enhanced by the choice of grid size; a finer grid ($64\times64\times64$) seems to reduce this effect.

Fig. 5 is, nevertheless, an excellent *ab initio* reconstruction of the electron density. Comparison with the 'true' phases shows that 90% of the phases were correctly determined, which is demonstrably sufficient to solve the structure. Many of the regions in the map have very low electron density, which suggests that the algorithm is having difficulty fitting the map. Despite this, a positive map consistent with the data has been found even though 10% of the phases were incorrectly determined. Similarly, inspection of the residuals $R[=(|F_k|-|D_k|)/\sigma_k]$ revealed no unusually large values which might have indicated that phases had been determined incorrectly.

The origin-defining reflections were chosen to be strong amplitudes near the origin of reciprocal space having the correct parity to determine the origin uniquely. No test was applied to consider how strongly correlated these structure factors were to other strong reflections. Such a 'convergence-mapping' technique has yet to be developed using MAXENT, but it should be able to find more powerful starting sets. This would in turn help to solve more complex structures.

The approach described above is not necessarily being proposed as a practical programme for solving centrosymmetric crystals. There is, for instance, no way of refining the phase predictions once made. The MAXENT map with 90% of the phases correctly determined is, nevertheless, superior to the conventional map using the 'true' phases. MAXENT yielded the correct structure from two arbitrarily chosen (though strong) origin-defining reflections, showing that it is more than a theorist's dream. A drawback is that wrong phase paths must be followed a long way before they are forbidden or appear unreasonable. This prevents the early pruning of the branches of the phase tree (Bricogne, 1984; Livesey, 1984).

3. The Bayesian approach to phase extension

A model map, which contain fragments of recognized structure, predicts phases and amplitudes for all the reflections, but we need a way for deciding which of these phase predictions to accept. Rather than the simple *ad hoc* rule of § 2, a more sophisticated Bayesian approach, consistent with the result derived by Woolfson (1956), is now described.

The structure factors of a crystal with electron density $\rho(\mathbf{r})$ are given by the Fourier transform

$$F(\mathbf{k})=\sum\rho(\mathbf{r})\exp(i2\pi\mathbf{k}\,.\,\mathbf{r}).$$

This electron density $\rho(\mathbf{r})$ may be conveniently decomposed into a contribution from the atoms that have already been located, and a contribution from the atoms as yet unlocated:

$$\rho(\mathbf{r})=\sum_{j=1}^{N}\rho_j(\mathbf{r})=\sum_{l=1}^{N_l}\rho_l(\mathbf{r})+\sum_{u=1}^{N_u}\rho_u(\mathbf{r}),$$

where $N=$ number of atoms in the unit cell, $l=$ located atom, $u=$ unlocated atom, and $\rho_j=$ electron density of the jth atom.

In terms of the Fourier transform $F(\mathbf{k})$ (or structure factors) we have

$$F(\mathbf{k})=F_l(\mathbf{k})+F_u(\mathbf{k}).$$

We now consider the contribution from individual atoms: because atoms are roughly the same shape, and do not significantly overlap, we can deconvolve the shape of the electron density and replace the atoms by delta functions at $\{\mathbf{r}_j\}$:

$$\rho_j(\mathbf{r})=Z_j\delta(\mathbf{r}-\mathbf{r}_j).$$

Then

$$F(\mathbf{k})=\sum_{\mathbf{r}}\sum_{j}\rho_j(\mathbf{r})\exp(i2\pi\mathbf{k}\,.\,\mathbf{r})$$
$$=\sum_{j}Z_j\exp(i2\pi\mathbf{k}\,.\,\mathbf{r}_j)$$

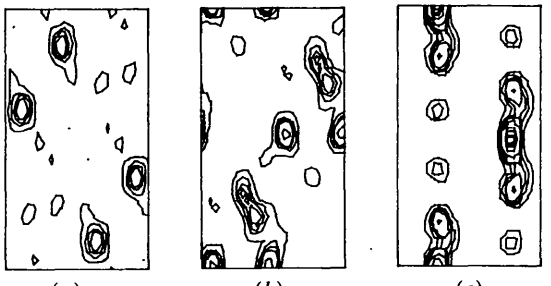

(a) (b) (c)

Fig. 5. The MAXENT map from 159 amplitudes with refined phases (Webster & Wood, 1981).

(a) (b) (c)

Fig. 6. The conventional Fourier map from 159 reflections and refined phases.

For the unlocated atoms $\{\mathbf{r}_u\}$ we know only their individual strengths of scattering, which are proportional to their atomic numbers $\{Z_u\}$, and not their positions, so $F_u(\mathbf{k})$ is the resultant of a sum of vectors with known magnitudes but unknown phases. Chemical knowledge such as bond lengths and bond angles would certainly constrain the phases further, but if we choose to ignore these considerations and assign the phases randomly we will obtain the following likelihood:

$$\text{prob}\,[F_u(\mathbf{k})|\{Z_u\}] \propto \exp\,[-|F_u(\mathbf{k})|^2/2\sigma^2],$$

where

$$\sigma^2 = \sum_{u=1}^{N_u} Z_u^2.$$

Although atoms are not really points, they are sufficiently small so that $\sigma = \sigma(\mathbf{k})$ is a slowly varying function of $\mathbf{k}$. We therefore approximate $\sigma^2(\mathbf{k})$ by $\langle\sigma^2\rangle$, where $\langle\sigma^2\rangle$ is a spherical average of the relevant atomic form factors over the $\mathbf{k}$ space of interest. With this approximation, and given the model, the likelihood that the $\mathbf{k}$th structure factor is $F(\mathbf{k})$ becomes

$$\text{prob}\,[F(\mathbf{k})|m(\mathbf{r}), \langle\sigma^2\rangle] \propto \exp\,[-|F_i(\mathbf{k}) - F(\mathbf{k})|^2/2\langle\sigma^2\rangle].$$

By comparison with other uncertainties, our intensities are measured to good accuracy, so we know that the magnitude of the $\mathbf{k}$th structure factor is $|D(\mathbf{k})|$. In the case of a centrosymmetric crystal such as TICLAC, the phases can only be 0 or π, so the predicted phase is simply 'right' or 'wrong'. Thus, given the model, we can calculate the probability that the true structure factor has the same phase as our model, but magnitude $|D(\mathbf{k})|$:

$$\text{prob}\,[F(\mathbf{k}) = |D(\mathbf{k})|, \arg(F_i(\mathbf{k}))|m(\mathbf{r}), \langle\sigma^2\rangle] \propto \exp\,[-(|F_i(\mathbf{k})| - |D(\mathbf{k})|)^2/2\langle\sigma^2\rangle].$$

We can also find the probability that the true structure factor is π out of phase with the model prediction:

$$\text{prob}\,[F(\mathbf{k}) = |D(\mathbf{k})|, -\arg(F_i(\mathbf{k}))|m(\mathbf{r}), \langle\sigma^2\rangle] \propto \exp\,[-(|F_i(\mathbf{k})| + |D(\mathbf{k})|)^2/2\langle\sigma^2\rangle].$$

The probability that the true (unmeasured) phase is the *same* as the model phase, therefore, is given by

$$\frac{\text{prob [true phase = model phase]}}{\text{prob [true phase = } -\text{model phase]}} = \exp\,[2|D(\mathbf{k})||F_i(\mathbf{k})|/\langle\sigma^2\rangle] = \exp\,(2\text{FOM}/\langle\sigma^2\rangle),$$

where FOM = model amplitude × measured amplitude.

For this centrosymmetric case, the *figure of merit* above (FOM) is a direct measure of the probability that our model phase is the true phase. For the more general case of the non-centrosymmetric crystal, the phase can lie anywhere between $\mp\pi$ and our predicted phase is not simply 'right' or 'wrong', but it is simple to show that this FOM is related to the variance of the true phase about the model prediction. FOM is, therefore, a measure of the reliability of a phase prediction in both cases, and hence a useful statistic in deciding which of the phase predictions to accept.

4. The inclusion of partial structure

In Figs. 2 and 3 (27 and 72 reflections used) the Sn atoms and their surrounding octahedra of Cl and O atoms were clearly recognizable as such, given the knowledge of the chemical formula. We used this basic chemical knowledge to see what further improvements we could make to the rate of convergence and quality of the electron density map.

The position of Sn, the heavy atom in TICLAC, is easily located: the *ab initio* solution shows that this can be uniquely deduced from the map constructed from the origin-defining structure factors (and their symmetry-related reflections), together with the knowledge of the allowable special positions in the space group. The phases predicted by a model map which contained only the tin atoms at their correct positions were ranked in descending order of their FOM (see above), so that the more reliable phase predictions were at the top of the list. We expected the number of correct predictions to be related to the proportion of correctly located atoms in our model. We adopted a simple rule of thumb and accepted the top SELECT fraction of the phase predictions, defined by

$$\text{SELECT} \simeq \frac{\sum Z(\text{located})}{\sum Z(\text{all})} = \frac{(\text{e}^-\text{ in located atoms})}{(\text{e}^-\text{ in the unit cell})}.$$

Table 2 shows the effect of using this FOM and selection criterion. As expected, the FOM ranking places the more reliable phase predictions at the top

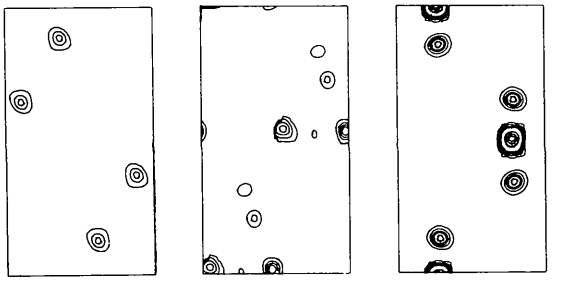

(*a*) (*b*) (*c*)

Fig. 7. The equivalent sections to Figs. 1-6 of the final MAXENT map after chemical knowledge had been assumed. The reconstruction was carried out on a 64×64×64 grid, using the top 60% of the 1196 measured amplitudes ranked according to their FOM from a model containing the previously located Sn and Cl atoms. (*a*) Section 1, (*b*) section 11, (*c*) section 17. [Contour levels (e Å^{-3}): 1·2, 2·2, 3·2, 4·2; 6, 34, 62, 90.]

Table 2. *Comparison of the 'true' phases with the model phases ranked according to a figure of merit,* FOM = *measured amplitude* × *model amplitude*

Selection criteria (What fraction of the phase predictions accepted)

Model (Located atoms)	SELECT $\left(\sim\frac{\sum Z(\text{located})}{\sum Z(\text{all})}\right)$
Sn	30%
Sn, Cl	50%
Sn, Cl O	60%
Sn, Cl, O, C	80%

Error comparison with data set (1) (159 reflections with $|h|$, $|k|$, $|l| \leq 5$)

Model	Fraction of data wrongly phased	Position of the first wrong prediction	Fraction of *selected* data wrongly phased
Sn	19/159	48%	0/50
Sn, Cl	21/159	56%	0/80
Sn, Cl, O	21/159	67%	0/95
Sn, Cl, O, C	15/159	77%	1/127

Error comparison with data set (2) (1196 reflections with $|h|$, $|k|$, $|l| \leq 16$)

Model	Fraction of data wrongly phased	Position of the first wrong prediction	Fraction of *selected* data wrongly phased
Sn	—	—	—
Sn, Cl	116/1196	25%	5/600
Sn, Cl, O	107/196	42%	7/720
Sn, Cl, O, C	78/1196	58%	11/960

of the list and the wrong predictions are pushed further down as more structure is incorporated into the model map.

The new structure-solving strategy is as follows: once Sn has been located, make a model map which is flat (with uniform ρ_e) apart from the Sn atoms. Use the top 30% of the FOM-ranked predictions to assign phases to the corresponding measured amplitudes and generate a MAXENT map on the basis of these data alone. This should enable us to locate more atoms (probably Cl, the next heaviest). Now use the predictions of a higher-order model, containing the Sn and Cl atoms, to assign phases to the top 50% of the data, make a better MAXENT map, and repeat the process.

This procedure was found to be very successful for TICLAC: the Sn+Cl model was sufficient to locate all the non-hydrogen atoms unambiguously. Fig. 7 shows the MAXENT reconstruction on a $64 \times 64 \times 64$ grid, using the top 60% of the 1196 measured amplitudes ($|h|, |k|, |l| \leq 16$), phased with an Sn+Cl model. The model map (which incorporates our prior chemical knowledge) and the FOM combine to give us some well phased data. In this way we circumvent the problems associated with the full phaseless problem, whilst the power of maximum entropy is used to tackle the problem of 'missing' data (with phases yet to be associated). We have found it better to use a fraction of the data that is reliably phased at any stage than to use a larger proportion with (say) 10% wrongly phased. The result is a high-quality electron density map of TICLAC.

We thank Dr M. Webster for providing us with data for TICLAC.

AKL thanks the Cavendish Trust Funds, St John's College and his parents for financial support during this work. The paper was written whilst he held an EMBO fellowship at Orsay, France.

DSS acknowledges financial support from the SERC.

References

BRICOGNE, G. (1984). *Acta Cryst.* **A40**, 410-445.

COLLINS, D. M. (1982). *Nature (London)*, **298**, 49-51.

GULL, S. F. & DANIELL, G. J. (1978). *Nature (London)*, **272**, 686-690.

GULL, S. F. & SKILLING, J. (1984). *IEE Proc.* **131F**, 646-659.

JAYNES, E. T. (1983). (Collected Works.) *Papers on Probability, Statistics and Statistical Physics*, edited by R. D. ROSENKRANTZ. Dordrecht: Reidel.

LIVESEY, A. K. (1984). PhD Thesis, Univ. of Cambridge.

LIVESEY, A. K. & SKILLING, J. (1985). *Acta Cryst.* **A41**, 113-122.

MILLER, G. A. & SCHLEMPER, E. O. (1978). *Inorg. Chim. Acta*, **30**, 131-134.

NAVASSA, J. (1985). *Acta Cryst.* **A41**, 232-244.

SKILLING, J. & BRYAN, R. K. (1984). *Mon. Not. R. Astron. Soc.* **211**, 111-124.

STEENSTRUP, S. & WILKINS, S. W. (1984). *Acta Cryst.* **A40**, 163-164.

WEBSTER, M. & WOOD, J. S. (1981). *J. Chem. Res. (M)*, pp. 0450-0456.

WOOLFSON, M. M. (1956). *Acta Cryst.* **9**, 804-810